

# Impedance spectroscopy on ceramic materials at high temperatures, considering stray fields and electromagnetic noise

T. M. Müller, J. Meinhardt, and F. Raether

Citation: *Rev. Sci. Instrum.* **84**, 015118 (2013); doi: 10.1063/1.4788733

View online: <http://dx.doi.org/10.1063/1.4788733>

View Table of Contents: <http://aip.scitation.org/toc/rsi/84/1>

Published by the [American Institute of Physics](#)

---

---

# Impedance spectroscopy on ceramic materials at high temperatures, considering stray fields and electromagnetic noise

T. M. Müller, J. Meinhardt, and F. Raether<sup>a)</sup>

*Fraunhofer Institute for Silicate Research ISC, Gottlieb-Keim-Str. 60, 95448 Bayreuth, Germany*

(Received 9 July 2012; accepted 7 January 2013; published online 30 January 2013)

Impedance spectroscopy of many ceramics is a challenge due to their high electrical resistance. Small disturbances can significantly alter the measuring results. In the present paper, it is shown how impedance measurements can be performed in an electromagnetically noisy ac furnace, using consequent Faraday shielding of the sample and the electrical connections. As example, the conductivity data of alumina was measured between room temperature and 1000 °C and compared to literature data. In addition, a correction method for the calculation of permittivity was developed to consider the stray fields in the sample-electrode setup. The distribution of the electrical field was simulated by finite element (FE) methods for different sample geometries and electrode arrangements. The deviations from the behavior of an ideal plate capacitor follow a linear trend and are in the order of 5% to 20% for an experimentally reasonable range of sample thicknesses. To check the theoretical results experimentally, alumina samples of varying thickness were measured. The customary calculation of permittivity leads to a clear trend with sample thickness, whereas the correction from the FE-simulation produces almost constant values of the relative permittivity. © 2013 American Institute of Physics. [<http://dx.doi.org/10.1063/1.4788733>]

## INTRODUCTION

Impedance spectroscopy (IS) is a well established method to measure the frequency dependent electrical behavior of materials.<sup>1</sup> It is particularly suitable for the non-destructive characterization of internal interfaces of the specimen under observation, such as the grain boundaries of ceramic samples. But, as it has been pointed out in detail by<sup>2</sup> and,<sup>3</sup> it is important to keep the experimental limitations of the IS method in mind. Especially the electrodes employed (material, placement, geometry) have a substantial effect on the measured properties.<sup>4,5</sup>

Special care is required if materials with high resistivity—like many ceramics—are to be measured. When a guardring is used to block surface currents,<sup>6</sup> several normalization equations (to correct for the sample geometry) have been proposed in literature.<sup>6–9</sup> They suggest effective diameters between the guardring's diameter and that of the enclosed electrode to calculate an effective electrode area to be used for normalization. Following these proposals, we encountered unreasonable discrepancies of the derived values when comparing measurements of the same sample with and without the use of the guardring: while the measured capacitance was nearly the same in both cases, the derived values of the relative permittivity in the guarded case differed about –36% from the unguarded ones. To overcome these problems, the ceramic capacitors were simulated in a three-dimensional finite element (FE) model. Comparing the simulated results with the equation of the ideal plate capacitor, a normalization factor was derived, which was applied to the experimental data to obtain material data independent from sample geometry.

Furthermore, when dealing with ceramics, the temperature dependencies of the electrical properties measured by IS are of special interest for many high temperature applications. Usually, when an electric heater is employed, dc currents are needed in order not to alter the electrical measurements by induction.<sup>6</sup> Special furnaces have been constructed for high temperature IS, which avoid any electromagnetic radiation in the interior. For that, electrical heating is done exclusively by DC current, and special temperature sensors are used.<sup>6,10</sup> But those furnaces are expensive and often very different from heating systems used in the application of the ceramics. Besides the furnace, there are other sources of electromagnetic noise in the laboratory, which have to be carefully eliminated. For that, metallic shields are usually used,<sup>10</sup> but they cannot withstand high temperatures. Therefore, we investigated an experimental setup that is capable of operating unbiased IS-measurements in irradiating environments at high temperatures.

## EXPERIMENTAL SETUP

Ceramic specimen were prepared by cold isostatic pressing of a commercial alumina powder (A16SG,  $d_{50} = 0.70 \mu\text{m}$ , Alcoa, Pittsburgh, USA) and sintering the cylindrical green bodies at 1550 °C for 2 h in air. After sintering, density—measured by the Archimedian method—was larger than 97% of theoretical density. This means that all residual pores are expected to be closed. The samples were cut and grinded to plane-parallel discs. Sample thicknesses were in the range of 300  $\mu\text{m}$  to 1000  $\mu\text{m}$ . Electrodes were applied by screen-printing a conductive platinum-paste (OS2: CL 11-5100, Heraeus, Germany). The paste was hardened at 1185 °C for 0.2 h. As alumina has a very low residual electric conductivity, a guardring is used to block surface currents.<sup>6</sup> Thus, only

<sup>a)</sup> Author to whom correspondence should be addressed. Electronic mail: [friedrich.raether@isc.fraunhofer.de](mailto:friedrich.raether@isc.fraunhofer.de). Tel.: +49-(0)921-786931-60. Fax: +49-(0)921-786931-61.

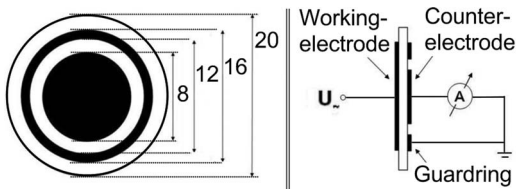


FIG. 1. Sample and electrode geometry applied by screen-printing (dimensions in mm).

the bulk properties of the ceramics are measured. Figure 1 shows the employed sample geometry. To obtain a proper electrical contact between the platinum layers and the measuring circuit, we used the platinum-paste (*OS2*) to glue thin Pt-wires ( $\varnothing = 100 \mu\text{m}$ ) to each electrode. These thin wires were clamped by alumina screws to the Pt-wires used in the sample chamber.

The IS measurements were carried out in the frequency range from 100 mHz to 1 MHz using an *Alpha-A Analyser* with *ZG4-Interface* (Novocontrol Technologies, Germany). The analyser allows to calibrate the impedances of the feed cables and connections of the measurement setup. A furnace (MoSi<sub>2</sub> heating elements from Kanthal AB Sweden, temperature control *2604* from Eurotherm Germany, atmosphere: air) was used to vary the sample temperature during IS measurements between ambient temperature and 1000 °C.

The thyristor activated temperature control, the ac current in the heating elements, and the laboratory environment provide crucial sources of electromagnetic emissions that may interfere with the electrical measurement by inducing voltage drops, e.g., along the rather long ( $\sim 0.5$  m) wires needed to contact the sample within the furnace. Therefore, a shielding is needed to ensure proper measurements. For this purpose, we used a ceramic casing (alumina) that was coated by electrically conductive platinum-paste (*FZ1137*, Fraunhofer IKTS, Germany; hardened at 1400 °C for 2.5 h). Additionally, platinum-wires placed within Pt-shielded alumina tubes connect the sample with the impedance analyser (see Figure 2). This way, we provide a closed—thermally and mechanically stable—Faraday cage along the complete signal chain.

Unfortunately, the shielding yields in temperature deviations inside and outside the shielded casing, which arise due to thermal isolation effects of the casing when the furnace temperature is changed rapidly. Thus, it is necessary to control

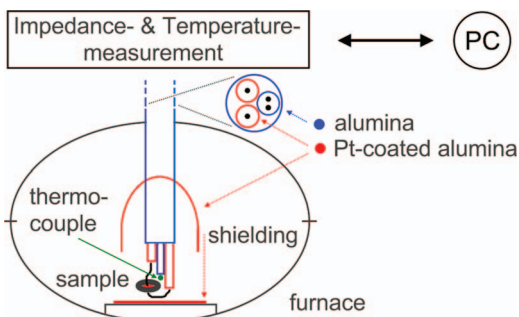


FIG. 2. Measurement system for the fully automatic recording of impedance spectra at temperatures from room temperature up to 1000 °C. The sample chamber (shielding) is shown in an open state here.

the sample temperature with a separate thermocouple, placed within the shielding directly adjacent to the sample. Figure 2 shows a sketch of the measurement system prepared within this work. A personal computer (PC) equipped with an in-house computer program (*VC++*) controls the heating and measuring process fully automatically (see Refs. 11 and 12 for further details).

## FE SIMULATION

With the equation of the ideal plate capacitor

$$C = \varepsilon_0 \cdot \varepsilon_r \cdot \frac{A}{d}, \quad (1)$$

where  $C$  is the capacitance,  $\varepsilon_0$  the vacuum permittivity,  $A$  the effective electrode area, and  $d$  the sample thickness, the relative permittivity of the sample  $\varepsilon_r$  can be calculated. The geometrical normalization factor  $dpA_{theo}$

$$dpA_{theo} = \frac{d}{A}. \quad (2)$$

( $dpA = d$  per  $A$ ) is calculated using the assumption that  $A = \pi/4 \times D_{CE}^2$ , where  $D_{CE}$  is the diameter of the counter electrode<sup>6</sup> (Figure 1). But due to stray fields, Eq. (1) is only accurate if  $(A/d) \rightarrow \infty$  and deviations for  $dpA_{theo}$  are expected with increasing sample thickness. Furthermore, when a guarding is used, effective diameters have been proposed in literature<sup>6-9</sup> that lead to unreasonable differences when comparing measurements of the same sample with and without guarding (see Introduction).

To overcome these discrepancies, FE-simulations of the three-dimensional electric field distributions resulting from the real sample geometry (in air) were carried out. The dielectric behaviour of the capacitor shown in Figure 1 was simulated using the FE software ANSYS 9.0 (ANSYS Inc., Canonsburg).<sup>13</sup> Sample thickness  $d$  was varied to quantify its effect on the calculated material properties.

Electrostatic simulations using the ANSYS element type *solid123* (material property = relative permittivity:  $\varepsilon_{air} = 1.00059$ ,  $\varepsilon_{ceramic} = 10$ ) were evaluated in terms of the resulting charge when a voltage of  $dU = 1$  V was applied between the working and the counter electrode (compare Figure 1). Figure 3 shows the geometrical model and the simulated electric potential when the guarding was used. Following these illustrations along the different geometries used within this work, it is seen on the computer display that the effective diameter of the electric field is always larger than that of the counter electrode. The use of the guarding reduces this effect.

Given the definition of the electrical capacitance

$$C := \frac{Q}{U}, \quad (3)$$

where  $Q$  is the electric charge of the electrode to which the voltage  $U$  is applied, the simulated geometrical normalization factor  $dpA_{SIM}$  was calculated as

$$dpA_{SIM} = \frac{\varepsilon_0 \cdot \varepsilon_r \cdot U}{Q(U, \varepsilon_r, A, d)}. \quad (4)$$

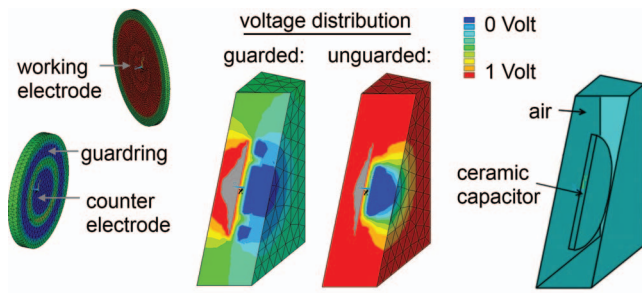


FIG. 3. Geometrical model of the ceramic capacitor within air (right) and electric potential calculated by FE methods (middle) when the electrode configuration with the guarding (left) was used (unguarded means that no constraints were applied to the nodes assigned to represent the guarding). The cross sections show the inside of the 3D-model.

A correction factor  $\delta$  was evaluated as

$$\delta := \frac{dpA_{theo}}{dpA_{SIM}} = \frac{Q \cdot d}{\epsilon_0 \cdot \epsilon_r \cdot U \cdot A} = \delta(d), \quad (5)$$

(with  $\epsilon_r = 10$  and  $U = 1$  V), which depends upon the sample thickness. Accordingly, the correction of the measured permittivity values is performed as

$$\epsilon_r \rightarrow \epsilon_r^{corrected}(d) = \epsilon_r \cdot \frac{1}{dpA_{theo}/dpA_{SIM}} = \frac{\epsilon_r}{\delta(d)}, \quad (6)$$

where  $\epsilon_r$  is calculated from the measured capacitance using Eq. (1).

The final FE-model holds about 68 000 to 320 000 elements, depending on the capacitors thickness  $d$ . The standard error of the simulation result  $\delta(d)$  due to convergence issues was determined to be around 2% (Figure 6).

## RESULTS AND DISCUSSION

First, the shielding of the electrical signal chain is tested. Figure 4 shows a comparison of electric signals with and without shielding, recorded with the help of a small antenna placed inside the sample chamber, and an oscilloscope. The rms values of the power density spectra (from 0 Hz to 25 MHz, sampling rate of 50 MHz) are

$$\begin{aligned} \text{rms (heating power 0\%, shielded)} &= 17.1 \mu\text{Vs}, \\ \text{rms (heating power 100\%, shielded)} &= 17.2 \mu\text{Vs}, \\ \text{rms (heating power 100\%, no shield)} &= 333 \mu\text{Vs}. \end{aligned}$$

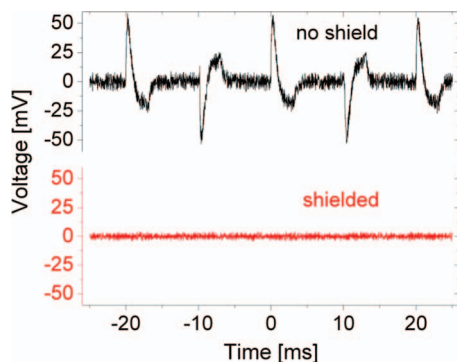


FIG. 4. Electromagnetic noise measurements within the sample chamber to test the shielding. The heating power of the furnace was 100% in both cases.

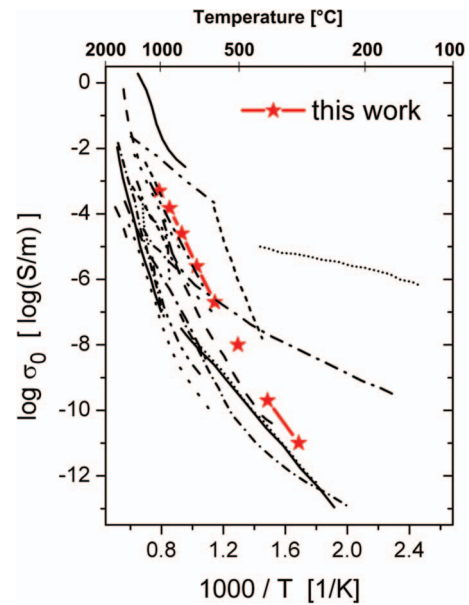


FIG. 5. Comparison of the conductivity data of alumina measured in this work with literature data from Ref. 14 (The references to the original measurements can be found in Ref. 15)

It is concluded that the technique described above yields an effective shielding against electromagnetic noise.

The electrical conductivity of alumina was measured from room temperature up to 1000 °C and compared to literature data. Figure 5 shows the corresponding Arrhenius plot. It can be seen that the values obtained with our experimental setup are in good agreement with literature data. The activation energy  $E_a$  of the dominant conduction mechanism is determined by the Arrhenius law

$$\sigma_0(T) = \frac{C}{T} \cdot \exp\left(-\frac{E_a}{k_B T}\right), \quad (7)$$

where  $\sigma_0$  is the (specific) conductivity,  $C$  is a constant,  $T$  is the absolute temperature in Kelvin, and  $k_B$  is Boltzmann's constant. Two temperature regions were identified with slightly different slope (Figure 5). The activation energies obtained for alumina by fitting Eq. (7) to the experimental data in these two regions were

$$E_a(319^\circ\text{C} - 455^\circ\text{C}) = (1.45 \pm 0.02) \text{ eV},$$

$$E_a(604^\circ\text{C} - 1009^\circ\text{C}) = (2.09 \pm 0.02) \text{ eV}.$$

This temperature dependency of the activation energy has been reported earlier in Ref. 4, where the values have been stated as:  $E_a(400^\circ\text{C} - 650^\circ\text{C}) = 0.9$  eV and  $E_a(650^\circ\text{C} - 1000^\circ\text{C}) = 2.0$  eV. The reason for the different behaviour at low and high temperatures is not clear, though leakage currents along the sample's surface have been suggested to contribute or even dominate at temperatures below 700 °C. But as a guarding was used within this work, surface currents were blocked, and leakage currents along the gas phase or the sample holder were ruled out through empty cell measurements.

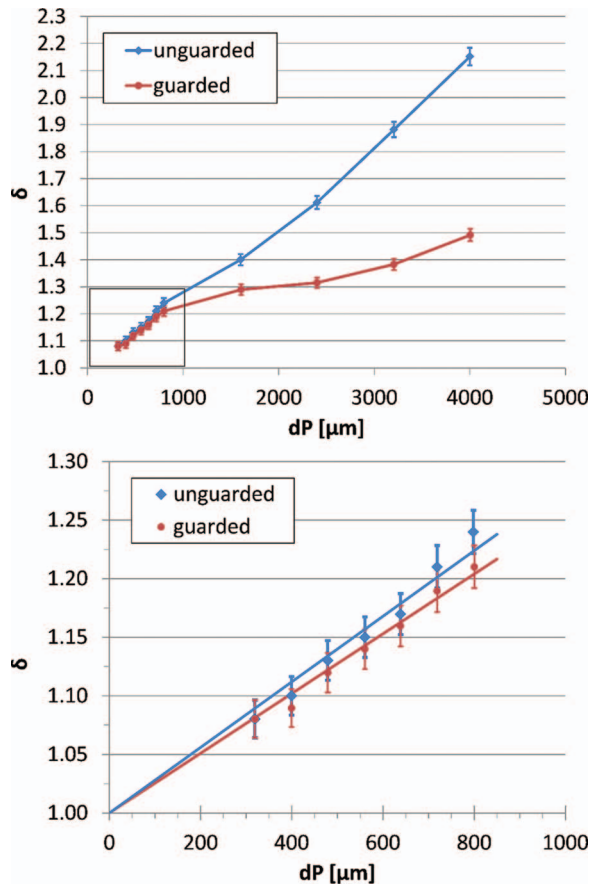


FIG. 6. Results of the FE simulations: correction factor  $\delta(d)$  as a function of the sample's thickness. The errorbars represent the uncertainty of the simulations due to convergence issues. The bottom part shows a zoomed view of the indicated region in the top part of the figure. (Fitting equation:  $y = 1 + m \cdot x$ . unguarded:  $m = (2.80 \pm 0.07) \times 10^{-4}$ . guarded:  $m = (2.55 \pm 0.04) \times 10^{-4}$ .)

Figure 6 shows the results of the FE simulations—evaluated with the correction factor  $\delta(d)$  defined in Eq. (5). Deviations from  $dP_{theo}$  up to 20% are observed. When the guarding is used, these deviations tend to be systematically smaller. For small  $d \leq 1$  mm,  $\delta(d)$  can be described as a simple linear function. With increasing thickness ( $d > 1$  mm), the curves become clearly nonlinear, especially the guarded one, and the difference between the guarded and the unguarded data further increases (see Figure 6).

Finally, we applied these results to the experimental permittivity data of alumina samples of varying thickness—measured at 1.2 MHz and room temperature—and compared the relative permittivity for standard and FE corrected geometrical normalization. As it can be seen in Figure 7, a clear trend of the permittivity data with sample thickness was detected after standard normalization. For the values obtained with the corrected normalization factors, this dependency on the sample thickness has been successfully eliminated.

These results show that, for standard capacitance measurements of ceramic substrates, a systematic error of 5% to 20% is to be expected. The deviations are much larger than uncertainties of the electrical measurements. So, the correction should always be applied, especially if samples of different geometries are to be compared.

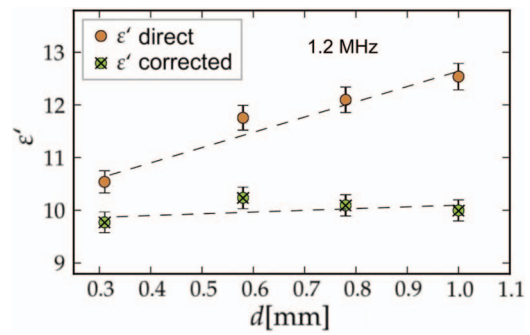


FIG. 7. Relative permittivity values of alumina measured at 1.2 MHz and room temperature (guarded configuration). The values stated as “direct” have been normalized using the standard geometrical factors, for the “corrected” ones the FE results have been applied.

## CONCLUSIONS

It was shown that the special shielding technique presented within this work successfully protects the electric measurements against electromagnetic radiation. It can be used in an electromagnetic noisy environment and withstands high temperatures. Although not tested in the current setup, maximum measuring temperatures of 1500 °C are expected for the technique. Moreover it was shown, that the FE simulation of the experimental setup can be used to correct stray fields, which otherwise lead to errors of 5% to 20% in a standard setup with plate capacitors. The use of the geometrical normalization factor that results from the FE simulations effectively eliminates this systematic error and therefore allows to calculate the material's properties independently of the geometry of the sample under investigation. The same FE model can also be used to obtain impedance data from samples of any geometry. So, the restriction to the standard plate geometry is overcome. However, when dealing with complex geometries at high frequencies, possible electrodynamic effects on the field distribution should be considered and scrutinized carefully.

## ACKNOWLEDGMENTS

The authors would like to thank A. Hardock and D. Biskupski for their help with the measurements, H. Schömig for the preparation of the ceramic samples, and the *Bayerische Forschungstiftung* for financial support within the joint project *FOROXID*.

- <sup>1</sup>J. Ross Macdonald and E. Barsoukov, *Impedance Spectroscopy: Theory, Experiment, and Applications*, 2nd ed. (Wiley, New Jersey, 2005), pp. 0-471-64749-7.
- <sup>2</sup>G. Hsieh, T. O. Mason, E. J. Garboczi, and L. R. Pederson, *Solid State Ionics* **96**, 153–172 (1997).
- <sup>3</sup>D. D. Edwards, J.-H. Hwang, S. J. Ford, and T. O. Mason, *Solid State Ionics* **99**, 85–93 (1997).
- <sup>4</sup>J. Öjjerholm, “Ionic transport of  $\alpha$ -alumina below 1000 °C: An in situ impedance spectroscopy study,” Licentiate thesis, Royal Institute of Technology Stockholm, Schweden, 2004.
- <sup>5</sup>J. Winkler, P. V. Hendriksen, N. Bonanos, and M. Mogensen, *J. Electrochem. Soc.* **145**(4), 1184–1192 (1998).
- <sup>6</sup>F. G. Will and K. H. Janora, *J. A. Ceram. Soc.* **75**(10), 2795–2802 (1992).

- <sup>7</sup>Deutsche Norm, IEC 93:1980, German version HD 429 S1:1983, *Prüfverfahren für Elektroisierstoffe: Spezifischer Durchgangswiderstand und spezifischer Oberflächenwiderstand von festen, elektrisch isolierenden Werkstoffen*, VDE Verlag GmbH, 1993.
- <sup>8</sup>D 150-98 (reapproved 2004), *Standard Test Methods for AC Loss Characteristics and Permittivity (Dielectric Constant) of Solid Electrical Insulation*, ASTM International, US.
- <sup>9</sup>D 257-99 (reapproved 2005), *Standard Test Methods for DC Resistance or Conductance of Insulating Materials*, ASTM International, US.
- <sup>10</sup>D 1829-90 (reapproved 1999), *Standard Test Method for Electrical Resistance of Ceramic Materials at Elevated Temperatures*, ASTM International, US.
- <sup>11</sup>T. M. Müller, "Computergestütztes Materialdesign: Mikrostruktur und elektrische Eigenschaften von Zirkoniumdioxid-Aluminiumoxid Keramiken," Ph.D. dissertation, Einzureichen bei der Bayerischen Julius-Maximilians-Universität Würzburg, 2012.
- <sup>12</sup>A. Hardock, *Impedanzspektroskopie an Zirkoniumdioxid-Aluminiumoxid-Keramiken* (Diplomarbeit, Julius-Maximilians Universität Würzburg, 2010).
- <sup>13</sup>W. Schätzing, *FEM für Praktiker – Band 4: Elektrotechnik* (Expert, Renningen, Germany, 2003).
- <sup>14</sup>C. C. Wang, S. A. Akbar, W. Chen, and V. D. Patton, *J. Mater. Sci.* **30**, 1627–1641 (1995).
- <sup>15</sup>A. A. Bauer and J. L. Bates, *Batelle Mem. Inst. Rept. BMI-1930*: 23, 1974.